This is a repository copy of *Temperature-Stable Dielectric Ceramics based on Na$_{0.5}$Bi$_{0.5}$TiO$_3$*.

White Rose Research Online URL for this paper:
http://eprints.whiterose.ac.uk/125454/

Version: Published Version

Temperature-stable dielectric ceramics based on $Na_{0.5}Bi_{0.5}TiO_3$

Aurang Zeb[a,b], Saeed ullah Jan[a,b], Faith Bamiduro[a], David A. Hall[c], Steven J. Milne[a]

[a] Advanced Engineering Materials, School of Chemical Engineering, University of Leeds, Leeds, LS2 9JT, UK
[b] Department of Physics, Islamia College Peshawar, KP, Pakistan
[c] School of Materials, University of Manchester, Manchester, M13 9PL, UK

A B S T R A C T

Multiple ion substitutions to $Na_{0.5}Bi_{0.5}TiO_3$ give rise to favourable dielectric properties over the technologically important temperature range $-55\,°C$ to $300\,°C$. A relative permittivity, ε_r, = 1300 ± 15% was recorded, with low loss tangent, $\tan\delta \leq 0.025$, for temperatures from $310\,°C$ to $0\,°C$, $\tan\delta$ increasing to 0.05 at $-55\,°C$ (1 kHz) in the targeted solid solution $(1-x)[0.85Na_{0.5}Bi_{0.5}TiO_3–0.15Ba_{0.8}Ca_{0.2}Ti_{1-y}Zr_yO_3]–xNaNbO_3$: x = 0.3, y = 0.2. The ε_r-T plots for $NaNbO_3$ contents x < 0.2 exhibited a frequency-dependent inflection below the temperature of a broad dielectric peak. Higher levels of niobate substitution resulted in a single peak with frequency dispersion, typical of a normal relaxor ferroelectric. Experimental trends in properties suggest that the dielectric inflection is the true relaxor dielectric peak and appears as an inflection due to overlap with an independent broad dielectric peak. Process-related cation and oxygen vacancies and their possible contributions to dielectric properties are discussed.

1. Introduction

There is an ongoing drive to develop lead-free dielectrics for capacitors for use in electronic systems that can operate at temperatures well above $200\,°C$ [1–19]. Applications include deep-well oil and gas exploration, defence and aerospace, and emerging power electronics technologies [1]. Most of these applications demand upper working temperatures between 200–300 °C, with a lower operating temperature of $-55\,°C$ [2,3]. High and stable relative permittivity combined with low dielectric loss tangent are basic requirements of the dielectric. Conventional core-shell ferroelectric-based barium titanate dielectrics with high and temperature-stable relative permittivity (ε_r), for use in Class II capacitors have upper operating temperatures of < 200 °C. [3].

A number of lead-free dielectric ceramics with a temperature-stable relative permittivity (variation within ± 15%) to temperatures in excess of 200 °C have been reported in recent years [3]. However the challenge of simultaneously extending performance to 300 °C whilst maintaining the Electronics Industries Alliance (EIA) specified minimum operating temperature of $-55\,°C$, in tandem with low dielectric loss and relative permittivity ε_r values exceeding 1000, remains a major research challenge. The majority of the > 200 °C dielectrics are based on relaxor ferroelectrics. In a classic relaxor ferroelectric such as $Pb(Mg_{1/3}Nb_{2/3})O_3$, compositional and charge disorder on the perovskite crystal lattice prevent the microscale electrostatic alignment of dipoles which occurs in a ferroelectric such as $BaTiO_3$. The concept of polar nanoregions is usually employed to account for the characteristic dielectric properties of a relaxor ferroelectric: a broad ε_r peak with frequency dispersion arises from thermally induced changes to dipole

size and coupling dynamics. However it has been shown that multiple lattice substitution on the A and the B sites of the perovskite ABO_3 lattice can supress the relaxor dielectric peak. This enables ± 15% stability in ε_r values to be achieved over wide temperature ranges, extending to high temperatures, > 200 °C [3–24]. The new heavily disordered relaxors, with a near-flat ε_r-T response, are referred to as 'temperature-stable relaxors' [3,6–10].

The properties of the majority of temperature stable relaxors can broadly be classified as: (a) materials which achieve high upper temperature limits of stable ε_r (e.g. 300–500 °C) with mid value ε_r ($\varepsilon_{r\ mid}$) values of 1000–1200 but with a minimum working temperature (e.g. 50–100 °C) well above the required EIA standard value of $-55\,°C$; (b) materials which achieve stable ε_r over the target $-55\,°C$ to 300 °C temperature range but have a modest ε_{rmid} value of ~ 450–500, which is detrimental to capacitor volumetric efficiency. Moreover, a number of materials have undesirably high dielectric loss tangents over at least part of the temperature range of stable ε_r [3].

Against this background there is a requirement to discover new and improved compositions which achieve a temperature range of stable and high relative permittivity from $-55\,°C$ to 300 °C and exhibit low dielectric losses across the full temperature range. Selecting $Na_{0.5}Bi_{0.5}TiO_3$ as the parent relaxor material for developing a flattened ε_r-T response by compositional engineering is a promising approach, given the high peak ε_r values of $Na_{0.5}Bi_{0.5}TiO_3$ [3–5,17–20]. Here we demonstrate that Zr-modification of a $Na_{0.5}Bi_{0.5}TiO_3$- $Ba_{0.8}Ca_{0.2}TiO_3$-$NaNbO_3$ solid solution produces a material which satisfies the target -55 to 300 °C temperature range of stability whilst possessing a moderately high $\varepsilon_{r\ mid}$ value of 1300, with very promising values of dielectric loss.
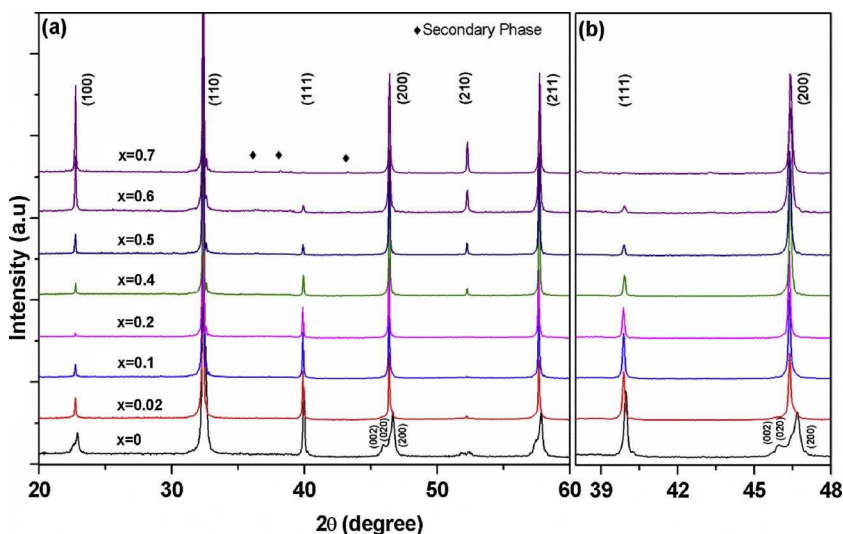
Fig. 1. (a) X-ray diffraction patterns of the ceramic series $(1-x)$ [0.85Na0.5Bi0.5TiO3–0.15Ba0.8Ca0.2TiO3]–xNaNbO3, $(0 \leq x \leq 0.7)$ (b) expanded scale showing {111} and {200} peaks. Diamond symbols indicate unidentified secondary phase(s) in $x = 0.06$ and 0.07 samples.

2. Experimental procedure

Multiple lattice substitutions to $Na_{0.5}Bi_{0.5}TiO_3$ involving Ca, Nb, and Zr were achieved in the solid solution system: $(1-x)$ $[0.85N_{0.5}Bi_{0.5}TiO_3–0.15Ba_{0.8}Ca_{0.2}Ti_{(1-y)}Zr_yO_3]–0.3NaNbO_3$ $(0 \leq x \leq 0.7; y = 0 \text{ or } 0.2)$. The solid solution nomenclature is abbreviated to 1-x(NBT-BCT)-xNN for $y = 0$ compositions (without Zr modification). This corresponds to the notional formula $1-x$ $(Na_{0.425}Bi_{0.425}Ba_{0.12}Ca_{0.03}TiO_3)–x(NaNbO_3)$, but the results described below indicate the products deviate from this composition.

Ceramic samples were prepared by a mixed oxide route, using the following starting reagents: $BaCO_3$ ($\geq$99% purity; Alpha Aesar, Ward Hill, MA); Nb_2O_5 (99.9%, Alpha Aesar); $CaCO_3$ ($\geq$99%; Sigma Aldrich, St. Louis, MO); Na_2CO_3 ($\geq$99.5%, Sigma Aldrich); Bi_2O_3 (99.9%, Aldrich); TiO_2 (99.9%, Aldrich) and ZrO_2 (99%, Sigma Aldrich). The raw powders were dried overnight in an oven at $\sim 200\,^{\circ}C$ prior to weighing in appropriate ratios, followed by ball milling in isopropanol for 24 h. The dried slurries were sieved through a 300 µm nylon mesh and calcined at 850 °C for 4 h (heating rate 5 °C/min). A binder (Ciba Glascol HA4; Ciba Speciality Chemicals, Bradford UK) was introduced and the powders were re-milled again for 24 h. These powders were uniaxially compacted in a steel die at ~ 70 MPa followed by cold isostatic pressing at 200 MPa to produce disc-shaped pellets, ~ 10 mm in diameter and ~ 1.5 mm thickness. The pellets were embedded in a previously calcined powder of the same composition in an alumina crucible, and a lid fitted to minimise loss of volatile components during sintering, carried out at a temperature 1160 °C, for 10 h (heating rate 1 °C/min to 550 °C, then 5 °C/min to 1160 °C; cooling rate 5 °C/min).

Phase analysis of the sintered pellets was performed on crushed pellets using a X-ray diffractometer (Bruker; D8, Karlsruhe, Germany, λ $_{Cu-K\alpha 1} = 1.5406$ Å, scan speed 1°/min): an external standard was used for calibration purposes prior to commencing the measurements. Microstructural analysis was carried out on fracture surfaces by scanning electron microscopy, SEM, which qualitatively indicated grain sizes of 2–6 µm. Ion polished surfaces were also examined by SEM (LEO Gemini 1530 Oxford instruments) with energy dispersive X-ray analysis EDX facility. Phase quantification (% area) was obtained from SEM-EDX maps by processing energy dispersive X-ray (EDX) area maps using Image J software (v1.50i).

For dielectric measurements, the sintered ceramics were polished using 400 and 800 grade silicon carbide papers and electrodes applied using silver paint (Agar Scientific, Stansted, UK); pellets were fired at 550 °C for 10 min to form the electrodes. Values of relative permittivity and loss tangent were measured as a function of temperature using an impedance analyser (HP Agilent 4192A, Hewlett Packard, Santa Clara,

CA). The influence of an electric bias field on the dielectric properties was determined by analysis of polarisation-electric field (P-E) loops using a field amplitude of 1 kV/mm. The required time-dependent voltage waveforms were generated using a HP33120A function generator and then applied to the specimens by means of a high voltage amplifier (Chevin Research, Otley, UK). Values of dc resistance were measured using a Keithley 617 programmable electrometer (Cleveland, OH) in the temperature range 250–550 °C at a fixed dc voltage of 80 V.

3. Results and discussion

Room temperature X-ray powder diffraction patterns of crushed sintered pellets of 1-x(NBT-BCT)-xNN formulations (without Zr modification) are shown in Fig. 1. The crystal structure of the parent NBT compound is complex, being a distorted perovskite with extensive oxygen tilt systems: it is reported to be rhombohedral or monoclinic at room temperature becoming tetragonal at 400 °C [26–29]. The lack of resolution in normal laboratory XRD data, Fig. 1, makes definitive phase analysis of NBT-BCT-NN challenging. The XRD patterns for compositions $x > 0.02$ appear to be pseudocubic, whilst sample $x = 0$ and possibly $x = 0.02$ appear to be mixed tetragonal and pseudocubic. There was a low intensity peak (32.4 °2θ) adjacent to the 110 main-phase perovskite peak in $x \geq 0.1$ samples. This corresponds to the most intense reflection in the XRD pattern of $NaNbO_3$ (ICDD 04-017-2917). Additional unidentified weak extra peaks appeared in $x = 0.6$ and 0.7 samples. There was no significant variation in cubic lattice parameter with increasing $NaNbO_3$ content, but the changes to dielectric data (Fig. 2) indicate that a change to the composition of the solid solution occurred with increasing x, consistent with $NaNbO_3$ incorporation.

The ε_r-T plots for sample compositions, $x = 0, 0.02, 0.05, 0.1$, each showed an inflection below the temperature of a broad peak: these are labelled T_1 and T_2 respectively, Fig. 2. This type of dielectric plot with a broad peak and a frequency dependent inflection is similar to that reported for unmodified $Na_{0.5}Bi_{0.5}TiO_3$ and for other $N_{0.5}Bi_{0.5}TiO_3$ solid solutions such as the Pb-free piezoelectric material NBT-BT [3–5,17,18]. The T_1 peak of the latter has been attributed in the literature to a depolarisation event, and T_2 labelled as T_m implying it to be a normal relaxor ferroelectric peak. However, the broad peaks around temperature T_2 in Fig. 2a–c showed negligible frequency dependence, unlike that of typical relaxors. Without $NaNbO_3$ modification ($x = 0$) the very broad T_2 peak was centred at $\sim 250\,^{\circ}C$; this reduced slightly to $\sim 220\,^{\circ}C$ for all of the $NaNbO_3$ modified compositions $x = 0, 0.02, 0.05$ and 0.1. The magnitude of the T_2 dielectric peak decreased with increasing x for the $x \leq 0.1$ compositional series and was barely detectable at composition $x = 0.2$, Fig. 2a–d. Because of the disappearance of
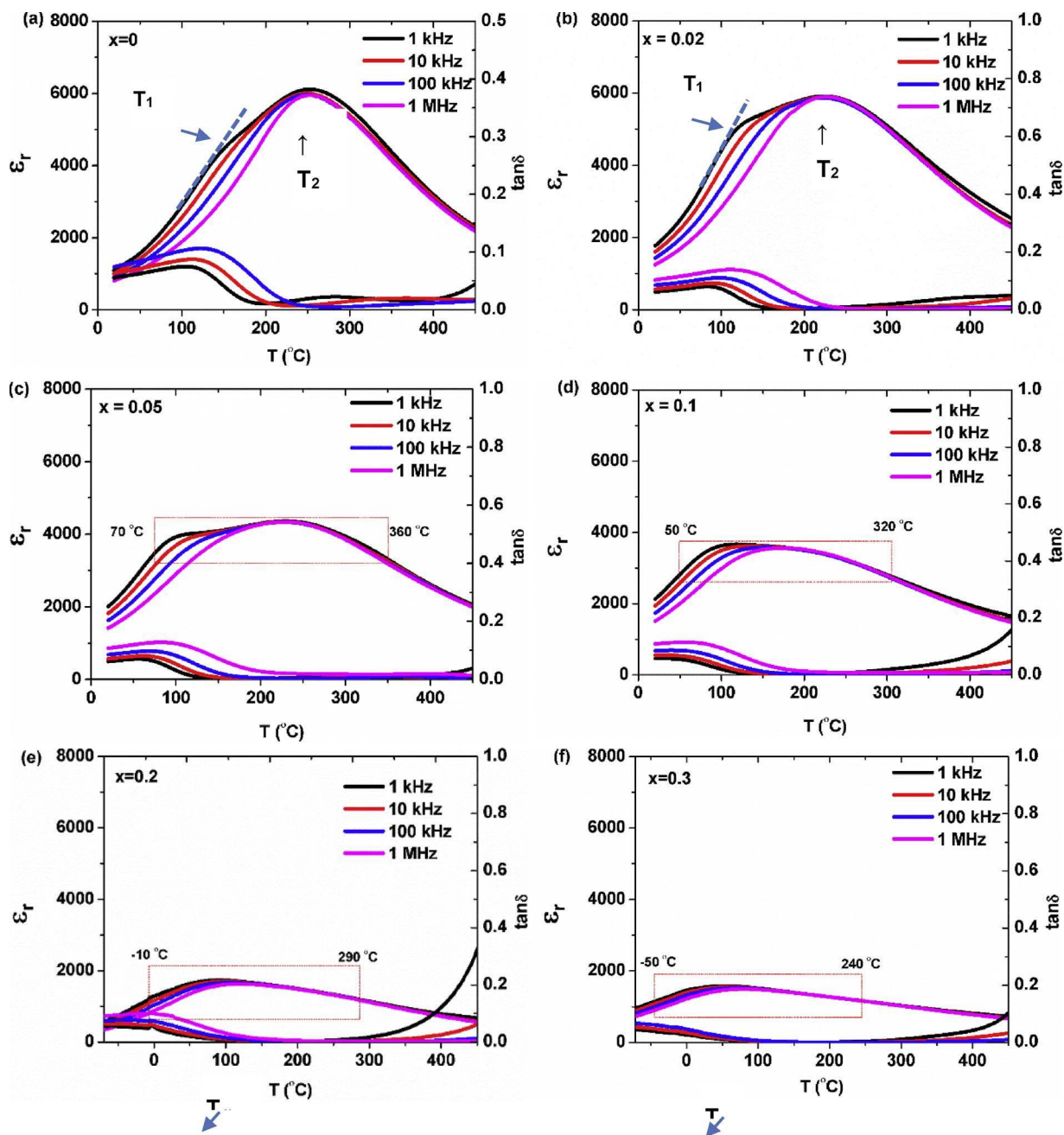
Fig. 2. Temperature-dependent relative permittivity, εr, and loss tangent, tanδ, of (1−x)[0.85Na0.5Bi0.5TiO3–0.15Ba0.8Ca0.2TiO3]–xNaNbO3: (a) x = 0 (expanded tanδ scale); (b) x = 0.02; (c) x = 0.05; (d) x = 0.1; (e) x = 0.2, (f) x = 0.3. Boxes indicates temperature range of ± 15% stability in εr. The 'inflection' and peak are labelled T1 and T2 (Fig. 3a, b.)

Table 1
Summary of the properties of $(1-x)[Na_{0.5}Bi_{0.5}TiO_3–0.15$ $Ba_{0.8}Ca_{0.2}TiO_3]–x[NaNbO_3]$ $(0 \le x \le 0.5)$ and Zr-modified ceramics, $0.7[Na_{0.5}Bi_{0.5}TiO_3–0.15Ba_{0.8}Ca_{0.2}Ti_{0.8}Zr_{0.2}O_3]–0.3[NaNbO]_3$, 'x = 0.3, y = 0.2' (1 kHz). * ε_{rmid} refers to the median value in the T range quoted for ε_r ± 15%.

x	$\varepsilon_{r25\,°C}$	T_1, T_m (°C)	T_2 (°C)	ε_{rmax}	ε_{rmid*}	T-range (°C) ε_{rmid} ± 15%	T-range (°C) tanδ ≤ 0.025
0	1190	160	250	6120	–	–	170 to 410
0.02	1870	120	220	5690	–	–	140 to 310
0.05	2110	110	220	4360	3800	70 to 360	110 to 420
0.1	2230	100	220	3630	3190	50 to 320	100 to 310
0.2	1530	*80*	–	1720	1500	−10 to 290	50 to 310
0.3	1550	*50*	–	1580	1400	−50 to 240	20 to 340
0.4	1460	*40*	–	1480	1300	−70 to 210	−10 to 380
0.45	1280	*30*	–	1280	1100	−70 to 200	−40 to 300
0.5	1100	*20*	–	1100	950	−70 to 190	−50 to 290
x = 0.3, y = 0.2	1480	*60*	–	1530	1300	−55 to 330	0 to 310
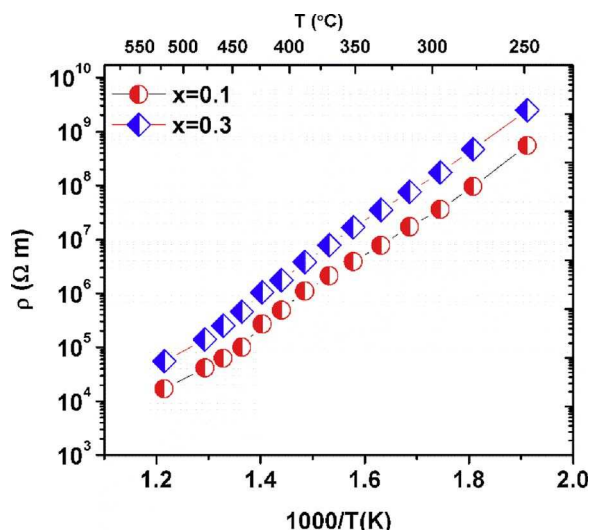
Fig. 3. dc resistivity versus reciprocal temperture for sample compositions x = 0.1 and 0.3.

Fig. 5. Temperature-dependence of relative permittivity (ε_r) of Zr-modified samples, x = 0.3, y = 0.2 ceramics: $0.7[0.85Na0.5Bi0.5TiO3–0.15Ba0.8Ca0.2Ti_{0.8}Zr_{0.2}O3]–0.3NaNbO3$. Dashed region indicates temperature range of ε_r with ± 15% stability.

the T_2 peak, the dielectric plots for samples x ≥ 0.2 were similar to those of a normal relaxor with a single frequency-dependent peak, labelled T_m. The observation that $NaNbO_3$ incorporation supresses the magnitude of the T_2 peak has been reported

The temperature ranges of ε_r ± 15% stability are represented by outline boxes in Fig. 2, and listed in Table 1 along with other dielectric data. At composition x = 0.3, ε_r = 1400 ± 15% at temperatures between −50 °C and 240 °C, with tanδ values ≤ 0.025 (1 kHz) for the temperature range 20 °C to 340 °C. None of these NBT-BCT-NN compositions satisfy the combination of basic dielectric properties required of a new generation of high temperature capacitor materials.
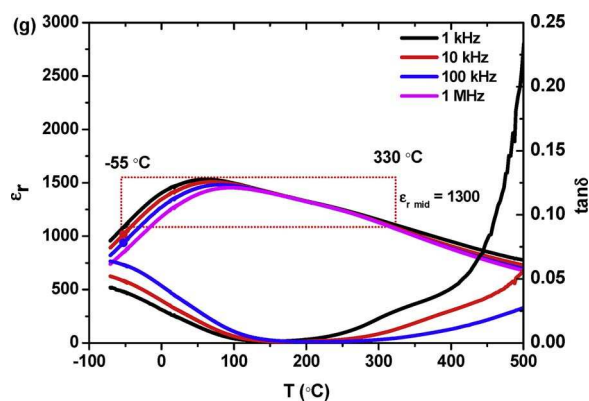
Values of d.c. resistivity were measured for sample x = 0.1 (twin dielectric anomalies, T_1 and T_2, but with a relatively small peak) and sample x = 0.3 (single relaxor peak, T_m). The plot of ρ vs. 1/T, shown in Fig. 3, indicates an activation energy for conduction of 0.5–0.6 eV, consistent with an oxide ion conduction mechanism. The x = 0.3 sample showed higher resistivity; at 300 °C, ρ = 2 × 10⁷ and 1 × 10⁸ Ωm for x = 0.1 and 0.3 respectively.

In order to further modify the solid solution composition NBT-BCT-NN with the aim of achieving improved dielectric performance, the effect of incorporating Zr^{4+} along with Ti^{4+} and Nb^{5+} ions on the B sites was investigated, selecting x = 0.3 as the base composition. The formulation $0.7[0.85Na_{0.5}Bi_{0.5}TiO_3–0.15Ba_{0.8}Ca_{0.2}Ti_{(1-y)}Zr_yO_3]–0.3NaNbO_3$ with y = 0.2 was selected for study. Higher values of $NaNbO_3$ content resulted in significant phase heterogeneity. Samples with x = 0.3, y = 0.2 were

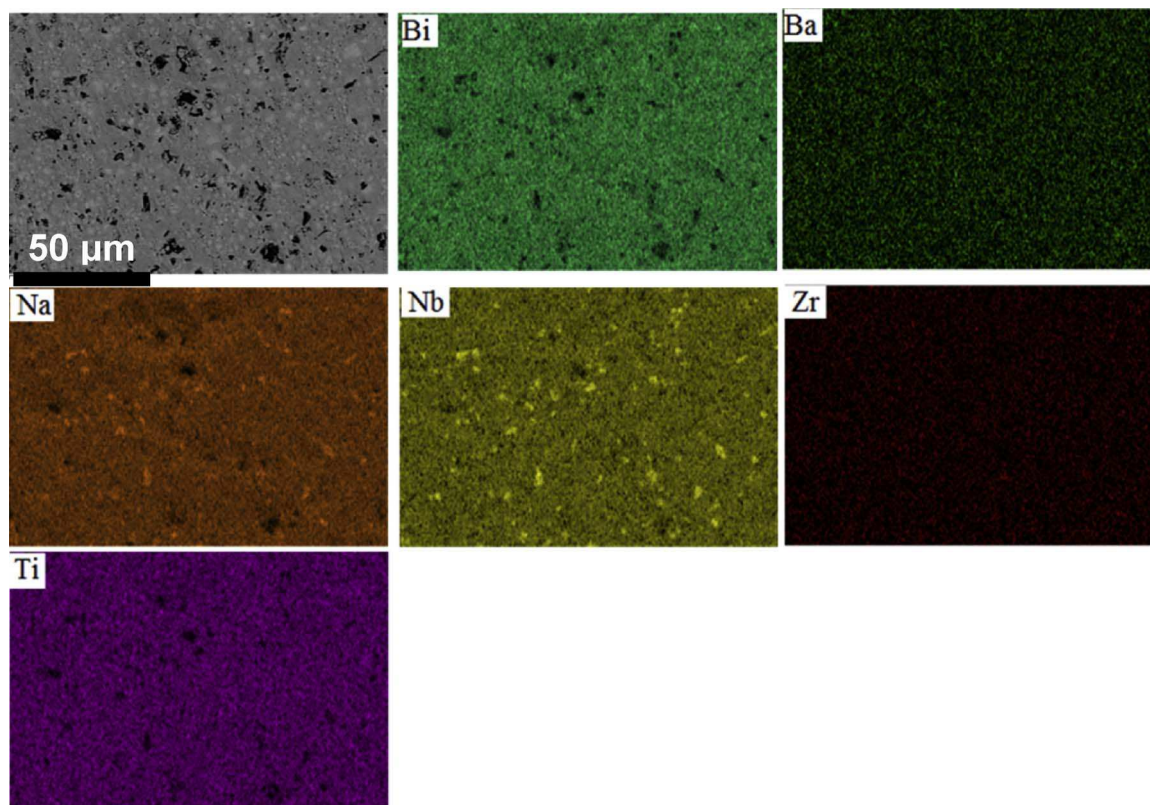**Fig. 4.** SEM-EDX mapping of x = 0.3, y = 0.2 ceramic: $0.7[0.85Na_{0.5}Bi_{0.5}TiO_3–0.15Ba_{0.8}Ca_{0.2}Ti_{0.82}Zr_{0.2}O_3]–0.3NaNbO_3$, illustrating the occurrence of a Na- and Nb-rich phase for this composition.

(a)

(b)
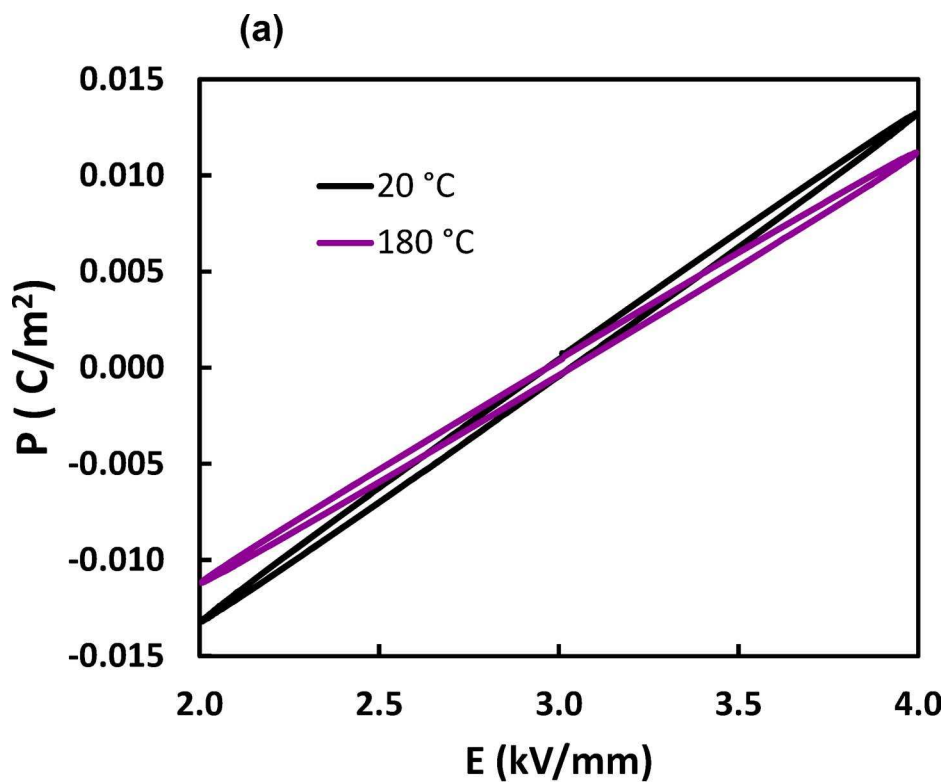
Fig. 6. (a) Examples of polarisation-electric field (P-E) loops used to obtain permittivity data at high fields; (b) variations in dielectric permittivity with increasing bias field for x = 0.3, y = 0.2: electric field amplitude, $E_o = 1\,kV/mm$, and frequency, f = 2 Hz.
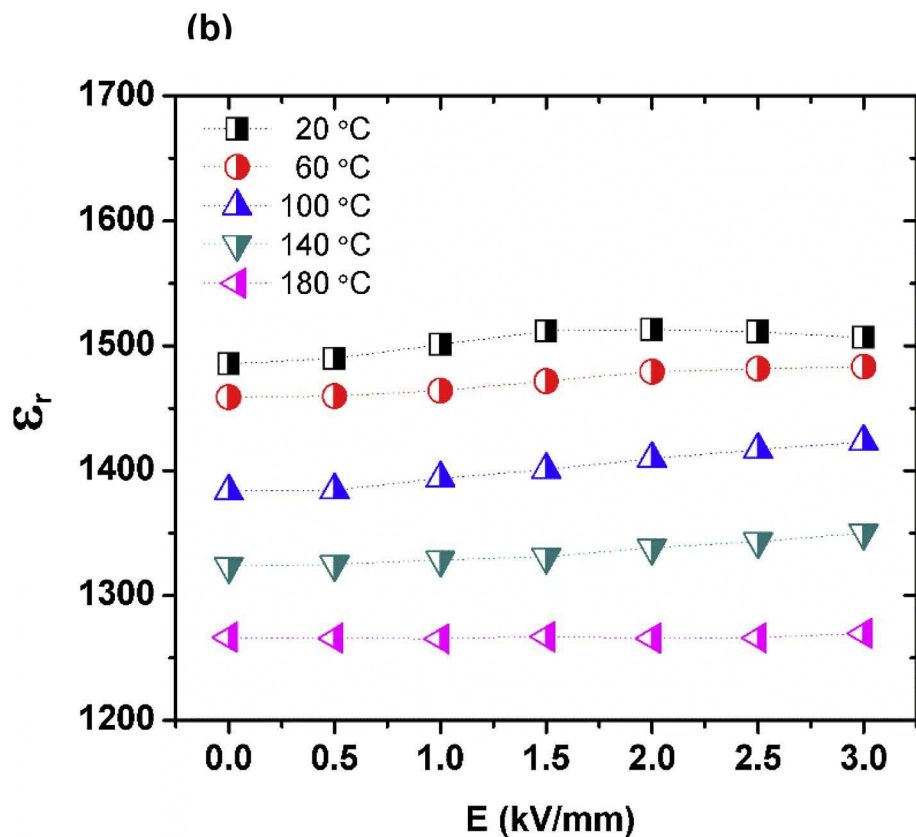
cubic by XRD, again showing evidence of a minor quantity of $NaNbO_3$, but with no other secondary peaks. However there was evidence from SEM-EDX of incomplete solid state reaction, in that grains of a Na- and Nb-rich phase were identified (Fig. 4). Image analysis of SEM-EDX maps indicated that this phase occupied ~10% of the area. As a consequence, the matrix will have a lower $NaNbO_3$ content than that of the notional composition. It is reasonable to assume that this secondary phase may also have been present in the unmodified NBT-BCT-NN materials, which would support the assignment that the extra XRD peak at 32.4 °2θ was due to $NaNbO_3$ (Fig. 1).

Fig. 7. Plot of T_1 (for x < 0.2) and T_m (for x ≥ 0.2) across the solid solution series (1–x) [0.85Na0.5Bi0.5TiO3–0.15Ba0.8Ca0.2TiO3]–x[NaNbO]₃. Estimated error in determining T_1 or T_m is ± 5 °C for compositions x = 0.02–0.5.
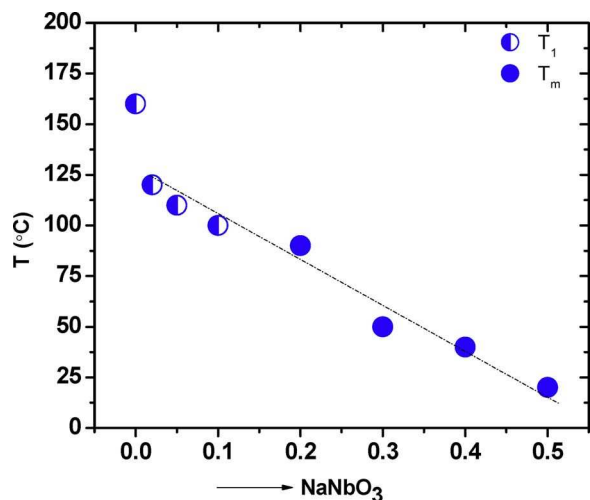
The ε_r -T plot for sample y = 0.2 indicated ε_{rmid} (150 °C) = 1300 ± 15% over the temperature range 330 °C to −55 °C with low dielectric loss, tanδ < 0.025, from 310 °C to 0 °C, Fig. 5. Below 0 °C, tan δ progressively increased to 0.05 as the temperature fell to −55 °C. This combination of properties offers an improvement in temperature-stability relative to the NBT-BCT-NN series, indicating the benefit of Zr incorporation. A combination of wide temperature-stable range of ε_r, encompassing the target −55 °C to 300 °C span, reasonably high ε_r values and low dielectric losses suggest that the x = 0.3, y = 0.2 composition is worthy of further development and testing as a high temperature capacitor material [3].

By way of property comparisons with related materials, $Na_{0.5}Bi_{0.5}TiO_3$–$BaTiO_3$–$NaTaO_3$ achieves a relative permittivity of ~1500 with good temperature-stability from −6 °C to 312 °C (based on a $\varepsilon_{r\,mid}$ value at 25 °C) and tan δ = 0.31 at 25 °C; the stability range is 3 °C to 284 °C for $\varepsilon_{r\,mid}$ of 125 °C [30]. For NBT-NN ceramics, a temperature-stable range of ε_r from −60 °C to 400 °C is reported, but tanδ appeared to increase to 0.05 at ~200 °C and to > 0.1 at ≥250 °C (1 kHz); the loss values below room-temperature were not reported [18]. The system $Na_{0.5}Bi_{0.5}TiO_3$–$BaTiO_3$–$NaNbO_3$ has also been studied and energy storage characteristics examined; the materials show an evolution in ε_r-T plots similar to that shown in Fig. 2 [17,19]. The $Na_{0.5}Bi_{0.5}TiO_3$-$Ba_{0.85}Ca_{0.15}Ti_{0.9}Zr_{0.1}O_3$ system is reported to give stable ε_r values from 81 °C to 330 °C [20]. Other reports of NBT based 'high temperature' dielectrics are reviewed in reference [3].

The mechanisms that supress the dielectric peak in compositionally-complex relaxor ferroelectrics are uncertain. The lattice is expected to be composed of a variety of different ABO_3 primary cell compositions, creating locally fluctuating electrostatic and strain fields where the length scales of fluctuations decrease with increases in concentration and multiplicity of substitutents. It seems that this variability in nanostructure restricts correlated cation displacements to an extent that the normal rise in permittivity, which creates a strong dielectric peak in a typical relaxor ferroelectric, is supressed. In the present work, the blocking effect of non-displaced Zr ions in ZrO_6 octaheda is expected to further disrupt polar ordering in the Zr-modified material relative to NBT-BCT. The experimental results (Fig. 5) illustrate that this additional disruption to polar order is important in terms of targeting temperature-stable dielectric properties over the −55 °C to 300 °C range. Furthermore, the NBT-BCT-NN materials are biphasic indicating only a proportion of the added NN is incorporated into the lattice. The role of displacements of Bi^{3+} ions in affecting the electrical properties of temperature stable relaxors is has yet to be established unequivocally

in this class of material. Mechanistic studies should include consideration of the role of cation and oxygen vacancy defects introduced during high temperature processing.

Because high temperature dielectric research programs are motivated by eventual use of the products as capacitor materials, which commonly take the form of thick films, a test of the stability in ε_r values under high d.c. bias fields was conducted, yielding the results presented in Fig. 6. It was found that the permittivity values remained stable under high electric field levels, with the most significant reductions arising as a result of temperature variations, consistent with the low-field dielectric measurements reported in Fig. 5. A similar result was observed previously for BCT-BMT [40] suggesting resiliance in ε_r under d.c. bias is a valuable characteristic of temperature-stable relaxor ferroelectric ceramics.

The double temperature-dependent dielectric anomalies in NBT and NBT-BaTiO₃ ceramics are similar to those for NBT-BCT-NN: x < 0.2. Their origin has been the subject of much scientific debate in the literature relating to the two former compositions. The broad frequency-independent peak at T_2 (Fig. 2) is often assigned to the true relaxor peak T_m, whilst the inflection at T_1 has been suggested to relate to depolarisation linked to a non-ergodic to ergodic relaxor ferroelectric transition. Transmission electron microscopy indicates that nanoscale R3c and P4bm phases co-exist over a wide–temperature range [31]. Based on this finding, other authors have suggested that the two dielectric anomalies can be attributed to the thermal evolution of these two different types of polar nanoregion [25].

Although the primary motivation for this research was to investigate temperature-stability of ε_r values as a function of composition in NBT-BCT-NN solid solutions, the observed experimental trends, together with an assessment of the data presented in previous reports, highlight the uncertainty over the origin of the double dielectric anomalies in NBT-based dielectrics. Fig. 7 shows how the inflection temperature, T_1, for samples with two dielectric anomalies (x < 0.02), and T_m, for the normal relaxor ferroelectric compositions (x ≥ 0.02), change as a function of the increasing NaNbO₃ content. A linear trend is observed, as reported for other relaxor ferroelectric solid solutions [7]. The linear correlation between T_1 (for low NaNbO₃ contents) and the unambiguously assigned T_m (for high NaNbO₃ contents) supports the view that the frequency-dependent inflection observed at T_1 represents the true relaxor ferroelectric peak. Further evidence that the inflection represents T_m lies in the position of the tanδ relaxation peak, which occurs at temperatures close to T_1 (Fig. 2): the tanδ relaxation peak is expected to occur at T ~ T_m in a relaxor ferroelectric.

Very diffuse, non–frequency dependent peaks of the type presented in Fig. 2a–c for T_2 can arise in a compositionally heterogeneous ferroelectric. However in NBT it appears that the gradation from an ergodic relaxor ferroelectric to a non-ergodic state occurs at or below the inflection temperature, T_1. Thus the T_2 peak cannot be associated with a diffuse ferroelectric phase transition- unless it were to arise from a separate phase, for example due to compositional segregation. It may well be that the T_2 peak somehow arises from evolution of two distinct polar nanoregions [25] and that by implication from Fig. 2 modification by NaNbO₃ produces a monophasic polar nanostructure, but other factors are worthy of consideration. Given that partial loss of Bi_2O_3 and Na_2O is very likely during high temperature ceramic processing there is the possibilty that lattice defects (cation and oxygen vacancies) contribute to the unusual ε_r-T response of NBT-based ceramics.

It has been demonstrated that donor doping of NBT by Nb causes a diminution of the 'T_2' peak, the extent of which depends on the level of Nb substitution [38,39]. Electrical conductivity in NBT originates from oxide ion conduction [38,39]. The effect of Nb^{5+} substitution for Ti^{4+} in NBT is to reduce the concentration of oxygen defects and reduce conductivity. The reasons for the similar dielectric and conductivity trends obsrved here for NaNbO₃ modified NBT-BCT to those reported for donor doped NBT, for example supression of the T_2 dielectric peak and increase in resistivity, are not understood. The NBT-BCT-NN

ceramic products are not single phase which indicates they do not conform to the notional formula 1-x($Na_{0.425}Bi_{0.425}Ti_{0.85}Ba_{0.12}Ca_{0.03}Ti_{0.15}O_3$)–x($NaNbO_3$). The correlations in electrical properties to donor doping (Nb-NBT) may imply that the substitution of Ti^{4+} by Nb^{5+} occurs without sufficient complementary charge balance on A sites by the extra Na^+ ions introduced from $NaNbO_3$. It has been reported there is a tendency for Na deficiency in NBT [41]. Moreover volatilisation losses are likely. Uncertainties over the Na (and Bi) contents may go some way to explaining the unexpected donor-like response of ceramics made from starting formulations containing extra Na_2CO_3, along with Nb_2O_5, as well as the possibility of differential volatilisation losses during prolonged high temperature sintering contributing to an apparent donor effect (from electrical property measurements), the thermodynamically stable solid solution formula may deviate from the assumed formula and therefore defect chemistry cannot be rationalised from the present set of results. Further work to identify if a single phase solid solution can be formed in the NBT-BCT-BCT 'ternary' system would help clarify this anomaly: even better dielectric properties may result from such an examination.

In terms of the double dielectrc anomalies, short range displacements of oxygen ions, changes to octahedral tilt systems and/or defect pair association phenomona are all aspects that require further investigation given the liklihood of oxygen, bismuth and sodium ion vacancies being introduced during high temperature processing. Oxygen vacancies introduced in this manner are not susceptible to re-oxidation by oxygen-annealing in contrast to 'intrinsic' oxygen vacancies [32]. However donor doping by Nb can have a compensating effect as has already been proven for NBT. There is evidence in the perovskite ferroelectrics literature that oxygen vacancies and defect pairs involving oxygen vacancies give rise to dielectric peaks (usually with frequency-dependent relaxation) at temperatures in the range reported for the T_2 peak in the NBT family [33–37]. Relatively little frequency-dependence in T_2 was observed for NBT-BCT-NN ($\sim 10\,°C$ variation over the frequency range from 100 Hz to 1 MHz). A more notable dispersion was observed in weak tanδ anomalies at $T \geq T_2$. In the field of fluorite solid oxide electrolytes cation defect-oxygen ion vacancy pair formation is considered to be responsible for a break in slope of Arrhenius plots [42,43]. A cation vacancy–oxygen vacancy extrinsic defect pair in NBT-ceramics could in principle associate in a similar manner. It is noted that Arrhenius plots for NBT show a change in activation energy for oxide conduction at temperatures close to T_2 [38,39]. Computational modelling has predicted the existence of ($V_{Bi}^{'''}$–$V_o^{\cdot\cdot}$) associates and ($Mg_{Ti}^{''}$ – $V_o^{\cdot\cdot}$) in Mg-modified NBT [44]. All of these observations confirm the many challenges faced in unravelling the complex structure-property relationships in the NBT family of dielectrics.

4. Conclusions

A study of the dielectric properties of compositionally modified $Na_{0.5}Bi_{0.5}TiO_3$ ceramics in the nominal solution system (1–x) [$0.85Na_{0.5}Bi_{0.5}TiO_3$–$0.15Ba_{0.8}Ca_{0.2}Ti_{1-y}Zr_yO_3$]–x$NaNbO_3$ ($0 \leq x \leq 0.8$, y = 0.2) indicate that stable relative permittivity develops over a wide temperature range with increasing levels of lattice substitutions. For NBT-BCT-NN a temperature-stable relative permittivity ε_r of $1400 \pm 15\%$ was observed for temperatures between $-50\,°C$ and $240\,°C$ for the composition x = 0.3, but from a device point of view further substitution of Ti^{4+} by Zr^{4+} led to even better performance, extending the range of temperature stability to $-55\,°C$ to $330\,°C$, with $\varepsilon_r = 1300 \pm 15\%$, accompanied by relatively low dielectric losses. This combination of properties achieves the Electronics Industries Alliance $-55\,°C$ lower temperature specification of a capacitor material, with moderately high relative permittivity and low dielectric loss, notably from $0\,°C$ to $300\,°C$. Compositional trends in relative permittivity- temperature plots and d.c. resistivity values suggested that a dielectric inflection is representative of a normal relaxor peak, T_m,

whilst the higher temperature peak is an independent feature. The role of cation-oxygen vacancies to the characteristic dielectric response of NBT-based ceramics is discussed.

References

[1] J. Watson, C. Castro, A review of high-temperature electronics technology and applications, J. Mater. Sci. Electron. 26 (2015) 9226–9235.

[2] J. Bultitude, J. McConnell, C. Shearer, High temperature capacitors and transient liquid phase interconnects for Pb-solder replacement, J. Mater. Sci. Electron. 26 (2015) 9236–9242.

[3] A. Zeb, S.J. Milne, High temperature dielectric ceramics: a review of temperature-stable high-permittivity perovskites, J. Mater. Sci. Electron. 26 (2015) 9243–9255.

[4] R. Dittmer, W. Jo, D. Damjanovic, J. Rodel, Lead-free high-temperature dielectrics with wide operational range, J. Appl. Phys. 109 (2011) 034107.

[5] R. Dittmer, E.M. Anton, W. Jo, H. Simons, J.E. Daniels, M. Hoffman, J. Pokorny, I.M. Reaney, J. Rödel, A high-temperature-capacitor dielectric based on $K_{0.5}Na_{0.5}NbO_3$-modified $Bi_{1/2}Na_{1/2}TiO_3$–$Bi_{1/2}K_{1/2}TiO_3$, J. Am. Ceram. Soc. 95 (2012) 3519–3524.

[6] A. Zeb, S.J. Milne, Stability of high-temperature dielectric properties for $(1-x)$ $Ba_{0.8}Ca_{0.2}TiO_3$–x$Bi(Mg_{0.5}Ti_{0.5})O_3$ ceramics, J. Am. Ceram. Soc. 96 (2013) 2887–2892.

[7] A. Zeb, Y. Bai, T. Button, S.J. Milne, Temperature-stable relative permittivity from $-70\,°C$ to $500\,°C$ in $(Ba_{0.8}Ca_{0.2})TiO_3$–$Bi(Mg_{0.5}Ti_{0.5})O_3$–$NaNbO_3$ ceramics, J. Am. Ceram. Soc. 97 (2014) 2479–2483.

[8] Q. Zhang, Z. Li, F. Li, Z. Xu, Structural and dielectric properties of $BaTiO_3$–Bi $(Mg_{0.5}Ti_{0.5})O_3$ lead-free ceramics, J. Am. Ceram. Soc. 94 (2011) 4335–4339.

[9] N. Raengthon, T. Sebastian, D. Cumming, I.M. Reaney, D.P. Cann, $BaTiO_3$-Bi $(Zn_{0.5}Ti_{0.5})O_3$-$BiScO_3$ ceramics for high-temperature capacitor applications, J. Am. Ceram. Soc. 95 (2012) 3554–3561.

[10] A. Zeb, S.J. Milne, Dielectric properties of $Ba_{0.8}Ca_{0.2}TiO_3$–$Bi(Mg_{0.5}Ti_{0.5})O_3$–$NaNbO_3$ ceramics, J. Am. Ceram. Soc. 96 (2013) 3701–3703.

[11] S. Wada, K. Yamato, P. Pulpan, N. Kumada, B.-Y. Lee, T. Iijima, C. Moriyoshi, Y. Kuroiwa, Peparation of barium titanate-bismuth magnesium titanate ceramics with high curie temperature and their piezoelectric properties, J. Ceram. Soc. Jpn. 118 (2010) 683–687.

[12] C. Xu, D. Lin, K.W. Kwok, Structure, electrical properties and depolarization temperature of $(Bi_{0.5}Na_{0.5})TiO_3$-$BaTiO_3$ lead-free piezoelectric ceramics, Solid State Sci. 10 (2008) 934–940.

[13] A. Zeb, S.J. Milne, Low variation in relative permittivity over the temperature range 25–450 °C for ceramics in the system $(1-x)[Ba_{0.8}Ca_{0.2}TiO_3]$–x$[Bi(Zn_{0.5}Ti_{0.5})O_3]$, J. Eur. Ceram. Soc. 34 (2014) 1727–1732.

[14] C. Kruea-In, G. Rujijanagul, F.-Y. Zhu, S.J. Milne, Relaxor behaviour of $K_{0.5}Bi_{0.5}TiO_3$-$BiScO_3$ ceramics, Appl. Phys. Lett. 100 (2012) 202904.

[15] S.U. Jan, A. Zeb, S.J. Milne, Dielectric ceramic with stable relative permittivity and low loss from -60 to 300 °C: a potential high temperature capacitor material, J. Eur. Ceram. Soc. 36 (2016) 2713–2718.

[16] A. Zeb, S.J. Milne, Temperature-stable dielectric properties from $-20\,°C$ to 430 °C in the system $BaTiO_3$–$Bi(Mg_{0.5}Z_{0.5})O_3$, J. Eur. Ceram. Soc. 34 (2014) 3159–3166.

[17] Q. Xu, M.T. Lanagan, W. Luo, L. Zhang, J. Xie, H. Hao, M. Cao, Z. Yao, H. Liu, Electrical properties and relaxation behavior of $Bi_{0.5}Na_{0.5}TiO_3$-$BaTiO_3$ ceramics modified with $NaNbO_3$, J. Eur. Ceram. Soc. 36 (2016) 2469–2477.

[18] X. Xu, et al., Ultra-wide temperature stable dielectric based on $Bi_{0.5}Na_{0.5}TiO_3$-$NaNbO_3$ system, J. Am. Ceram. Soc. 98 (2015) 3119–3126.

[19] Q. Xu, et al., Enhanced energy storage properties of $NaNbO_3$ modified $Bi_{0.5}Na_{0.5}TiO_3$ based ceramics, J. Eur. Ceram. Soc. 35 (2015) 545–553.

[20] Y. Pu, M. Yao, H. Liu, T. Frömling, Phase transition behaviour, dielectric and fer-roelectric properties of $(1-x)(Bi0.Na0.)TiO_3$-x$Ba_{0.85}Ca_{0.15}Ti_{0.9}Zr_{0.1}O_3$ ceramics, J. Eur. Ceram. Soc. 36 (2016) 2461–2468.

[21] Z. Liu, H. Fan, S. Lei, X. Ren, C. Long, Duplex structure in $K_{0.5}Na_{0.5}NbO_3$-$SrZrO_3$ ceramics with temperature-stable dielectric properties, J. Eur. Ceram. Soc. 37 (2017) 115–122.

[22] Z. Liu, H. Fan, M. Li, High temperature stable dielectric properties of $(K_{0.5}Na_{0.5})_{0.985}Bi_{0.015}Nb_{0.99}Cu_{0.01}O3$ ceramics with core-shell microstructures, J. Mater. Chem. C 3 (2015) 5851–5858.

[23] J. Shi, H. Fan, X. Liu, Y. Ma, Q. Li, Bi deficiencies induced high permittivity in lead-free BNBT-BST high-temperature dielectrics, J. Alloys Compd. 627 (2015) 463–467.

[24] X. Liu, H. Fan, J. Shi, Q. Li, Origin of anomalous giant dielectric performance in novel perovskite: $Bi_{0.5-x}La_xNa_{0.5-x}Li_xTi_{1-y}M_yO_3$ (M = Mg^{2+}, Ga_{3+}), Sci. Rep. 5 (2015) 12699.

[25] J. Wook, S. Schaab, E. Sapper, L.A. Schmitt, H.-J. Kleebe, A.J. Bell, J. Ro¨del, On the phase identity and its thermal evolution of lead free $(Bi_{1/2}Na_{1/2})TiO_3$-6 mol% $BaTiO3$, J. Appl. Phys. 110 (2011) 074106.

[26] I. Levin, I.M. Reaney, Nano and mesoscale structure of $Na_{0.5}Bi_{0.5}TiO_3$: a TEM perspective, Adv. Funct. Mater. 22 (2012) 3445–3452.

[27] E. Aksel, et al., Monoclinic crysatal structure of polycrystalline $Na_{0.5}Bi_{0.5}TiO_3$, Appl. Phys. Lett. 98 (2011) 152901.

[28] L.A. Schmitt, H.-J. Kleebe, Single grains hosting two space groups—a transmission electron microscopy study of a lead-free ferroelectric, Funct. Mater. Lett. 03 (2010) 55–58.

[29] D.S. Keeble, E.R. Barney, D.A. Keen, M.G. Tucker, J. Kreisel, P.A. Thomas, Bifurcated polarisation rotation in bismuth-based piezoelectrics, Adv. Funct. Mater. 23 (2013) 185–190.

[30] Q. Xu, et al., Structure and electrical properties of lead-free $Bi_{0.5}Na_{0.5}TiO_3$-based ceramics for energy storage applications, RSC Adv. 6 (2016) 59280–59291.

[31] V. Dorcet, G. Trolliard, P. Boullay, The structural origin of the antiferroelectric properties and relaxor behaviour of $Na_{0.5}Bi_{0.5}TiO_3$, Chem. Mater. 20 (2008) 5061.

[32] G. Sing, V.S. Tiwari, P.K. Gupta, Role of oxygen vacancies on relaxation and conduction behaviour of $KNbO_3$ ceramic, J. Appl. Phys. 107 (2010) 064103.

[33] C. Ang, Z. Yu, L.E. Cross, Oxygen-vacancy-related low-frequency dielectric relaxation and electrical conduction in $Bi:SrTiO_3$, Phys. Rev. B 62 (2000) 228–236.

[34] M. Li, et al., Dramatic influence of A-site nonstoichiometry on the electrical conductivity and conduction mechanisms in the perovskite oxide $Na_{0.5}Bi_{0.5}TiO_3$, Chem. Mater. 27 (2015) 629–634.

[35] W. Cao, et al., Defect-dipole induced large recoverable strain and high energy storage density in lead-free $Na_{0.5}Bi_{0.5}TiO_3$-based systems, Appl. Phys. Lett. 108 (2016) 202902.

[36] C. Cheon, et al., Role of $Bi_{0.5}K_{0.5}TiO_3$ in the dielectric relaxations of $BiFeO_3$-$Bi_{0.5}K_{0.5}TiO_3$, J. Appl. Phys. 119 (2016) 154101.

[37] Z. Wang, X.M. Chen, X.Q. Liu, Dielectric abnormalities of complex perovskite $BaFe_{0.5}Nb_{0.5}O_3$ ceramics over broad temperature and frequency range, Appl. Phys. Lett. 90 (2007) 022904.

[38] M. Li, L. Li, J. Zhang, D.C. Sinclair, Donor-doping and reduced leakage current in Nb-doped $Na_{0.5}Bi_{0.5}TiO_3$, Appl. Phys. Lett. 106 (2015) 102904.

[39] L. Li, Oxide Ion Conduction in A Site Bi-Containg Perovskite–Type Ceramics, PhD Thesis, University of Sheffield, 2016.

[40] A. Zeb, Lead-Free Dielectric and Piezoelectric Cewramics. PhD Thesis, University of Leeds, 2015.

[41] M. Spreitzer, M. Valant, D. Suvorov, Sodium deficiency in $Na_{0.5}Bi_{0.5}TiO_3$, J. Mater. Chem. 17 (2007) 185–192.

[42] V. Butler, C.R.A. Catlow, B.E.F. Fender, J.H. Harding, Dopant ion radius and conductivity in cerium dioxide, Solid State Ionics 8 (1983) 109–113.

[43] Y.S. Zhen, S.J. Milne, R.J. Brook, Oxygen ion conduction in CeO2 simultaneously doped with Y_2O_3 and Gd_2O_3, Sci. Ceram. 14 (1988) 1025–1030 Ed. D. Taylor, Institute of Ceramics.

[44] K.-C. Meyer, K. Albe, Influence of phase transitions and defect associates on the oxygen migration in the ion conductor $Na_{0.5}Bi_{0.5}TiO_3$, J. Mater. Chem. A 5 (2017) 4368–4375.